第 29 卷第 3 期
2013 年 3 月

无 机 化 学 学 报
CHINESE JOURNAL OF INORGANIC CHEMISTRY

Vol.29 No.3
628-634

用纤维素分散 ZnAl-LDHs 纳米片提高磷吸附性能

张燕茹[1] 梁杜娟[1] 吴 敏*,[2] 赵新华[1] 杨晓晶*,[1]
([1]北京师范大学化学学院,北京 100875)
([2]中国科学院理化技术研究所,北京 100080)

摘要：为了利用大比表面积性质,将锌铝层状双金属氢氧化物(ZnAl-LDHs)在甲酰胺中剥离,所得纳米片由纤维素稳定即在水溶液中不发生配列。通过 XRD、FTIR、SEM、TEM、元素分析、ICP 和离子色谱等手段研究了 ZnAl-LDHs 纳米片与羧甲基纤维素复合体的结构、组成和形貌,并探讨了纳米片的除磷性能。结果表明复合体对磷酸二氢根离子有很高的选择吸附性和较大的吸附量,吸附量最大约为 40 mg(P)·g^{-1} (LDHs)。

关键词：层状化合物；纳米片；胶体；吸附；磷
中图分类号：O614.24+1；O614.3+1　　**文献标识码**：A　　**文章编号**：1001-4861(2013)03-0628-07
DOI: 10.3969/j.issn.1001-4861.2013.00.069

Dispersion of ZnAl-LDHs Nanosheets by Cellulose to Improve Adsorption Capacity toward Phosphate

ZHANG Yan-Ru[1] LIANG Du-Juan[1] WU Min*,[2] ZHAO Xin-Hua[1] YANG Xiao-Jing*,[1]
([1]*College of Chemistry, Beijing Normal University, Beijing* 100875, *China*)
([2]*Technical Institute of Physics and Chemistry, Chinese Academy of Sciences, Beijing* 100080, *China*)

Abstract: In order to take advantage of large specific surface area, the nanosheets obtained by delaminating ZnAl layered double hydroxides (ZnAl-LDHs) in formamide were stabilized by cellulose in aqueous solution. The structure, composition and morphology of the resulting nanocomposites of ZnAl-LDHs nanosheets and carboxymethyl cellulose were characterized by XRD, FTIR, SEM, TEM, C, H, and N elemental analysis, ICP and ion chromatograph techniques. In addition, the performance of ZnAl-LDHs nanosheets on phosphorus removal was investigated. The results show that the nanocomposites have high selectivity and adsorption capacity toward phosphate. The selectivity sequences are as follows: $H_2PO_4^-$>>SO_4^{2-}>Cl^->NO_3^-. The maximum adsorption capacity could reach 40 mg of P per gram of LDHs approximately.

Key words: layered compounds; nanosheets; colloids; adsorption; phosphorus

0 Introduction

Inorganic nanosheets (INS) of the 2D crystals obtained by delamination of layered inorganic metal oxides and hydroxides have been studied extensively[1-7], and have attracted more attention due to the development of graphene research. INS usually exist with their delamination solvent as a colloidal suspension, thus drying or introducing of flocculants, etc. could cause the destruction of the colloidal system, i.e. restacking process takes place to produce 3D crystals. Therefore, in order to study the unique

收稿日期:2012-08-16。收修改稿日期:2012-09-30。
北京市自然科学基金(No.2112022)、国家自然科学基金(NSFC51172247, 5100381 和 20904064)资助项目。
*通讯联系人。E-mail:yang.xiaojing@bnu.edu.cn;Tel.: +861058802960;Fax: +861058802075;会员登记号:S060015134P。

properties of INS, INS must be separated from the liquid, it may be necessary to prepare even a unilamellar film by a layer-by-layer (LbL)[8] or by Langmuir-Blodgett (LB)[9] method; on the other hand, much more efforts have been devoted to constructing nanocomposites or superlattice layered compounds using INS as building blocks[10-12], by means of, commonly, the LbL method.

ZnAl-layered double hydroxides (LDHs) can be delaminated in formamide, like MgAl-LDHs[7]. The INS colloidal suspension of LDHs will flocculate in aqueous system, but this can be avoided by introducing a polymer, *i.e.* the interaction of the polymer and the INS can stabilize the dispersion state[13]. LDHs and their calcined poroducts exhibit a highly selective absorption toward phosphate[14-16]. The high selectivity is important since phosphate as well as nitrogen in water can cause the eutrophication even in a small concentration, *e.g.* 0.03 $mg \cdot L^{-1}$ phosphate would lead to red tides[17], and the phosphate removal will be disturbed by other coexisted anions. The adsorption mechanism of ZnAl-LDHs is probably ligand complexation or electrostatic attraction on the surface of the adsorbents[15]. Thus, the greater the surface area of the adsorbents, the more the sites available for the complexation, and the larger the adsorption capacity. Reducing the size of ZnAl-LDHs particles is certainly a way to improve the capacity. However, the INS of ZnAl-LDHs has the maximum specific surface area of the material. Accordingly, this work attempts to optimize phosphate uptake property of Zn-Al LDHs from aqueous solution, by stabilizing ZnAl-LDHs INS using cellulose. The results for the INS-containing composites show that no change in the selectivity toward phosphate is found, but a marked increase in the adsorption capacity is evident.

1 Experimental

1.1 Sample synthesis

All the reagents used were analytical grade. $NaNO_3$, NaH_2PO_4, NaCl, Na_2SO_4 and $ZnCl_2$ were obtained from Xilong Chemical Co., Ltd.; and $AlCl_3 \cdot 6H_2O$, urea formamide, and Carboxymethyl cellulose (CMC) sodium salt (Acros, MW=90,000, degrees of substitution=0.7), from Sinopharm Chemical Reagent Beijing Co. Ltd., Beijing Chemical Plant, Tianjin Bodi Chemical Co. Ltd, and Sigma-Aldrich Sigma-Aldrich Co. LLC., respectively.

CO_3^{2-} type ZnAl-LDHs precursor was synthesized by homogeneous precipitation method as reported[15]. In a flask, a mixed aqueous solution (0.8 L) containing 10 $mmol \cdot L^{-1}$ Zn^{2+}, 5 $mmol \cdot L^{-1}$ Al^{3+}, and 35 $mmol \cdot L^{-1}$ urea was heated at 100 ℃ under continuously magnetically stirring for 24 h. The precipitate was filtered, washed, and then dried in air. From the CO_3^{2-} type LDHs (1 g), NO_3^- LDHs was obtained via a salt-acid mixed solution treatment by using 1L aqueous solution containing 2 $mol \cdot L^{-1}$ $NaNO_3$ +9 $mmol \cdot L^{-1}$ HNO_3, in a N_2 atmosphere[15].

The NO_3^--LDHs (0.1 g) was added into formamide (100 mL) and then stirred for 24 h. Into the obtained nanosheets colloidal suspension, a solution of 0.067 0 g of CMC in formamide (50 mL) prepared as reported previously [13], was poured. In the present case, the charge number ratio of CMC to LDHs nanosheets, referred to as $R_{CMC/LDH}$, was 1; different amounts of CMC were designed with the ratio of 1/2, 1/4, 1/8, 1/16, and the samples were correspondingly called R-1, R-1/2, etc. After being stirred for 4 h, the suspension was centrifuged. The solid samples were water-washed several times until formamide was removed completely, as confirmed by non-existence of the stretching vibrations of C=O and C-N, respectively, at 1690 and 1312 cm^{-1} [13], in Fourier transform infrared (FTIR) spectrum (Fig.3) and then dried at 40 ℃ in vacuum.

1.2 Phosphate adsorption

The K_d values of different anions were determined and calculated using the following equation: K_d ($mL \cdot g^{-1}$)=anion adsorbed in solid ($mg \cdot g^{-1}$) /(anion concentration in solution ($mg \cdot mL^{-1}$). The wet composite sample containing 0.11 g NO_3^--LDHs was immersed in 25 mL of the mixed solution: 2$mmol \cdot L^{-1}$ NaCl +2 $mmol \cdot L^{-1}$ $NaNO_3$ +2 $mmol \cdot L^{-1}$ Na_2SO_4 +2 $mmol \cdot L^{-1}$ NaH_2PO_4 for 3 d with shaking. After being centrifuged, the supernatant solution was subjected to

ion chromatograph (Dionex DX-600).

The capacity of phosphate adsorption was measured by immersing the wet composite samples (0.05 g NO_3^--LDHs exfoliated) in a 2 mmol·L^{-1} NaH_2PO_4 solution (150 mL) with shaking for 3 d, which is longer than the period to reach the equilibration of the adsorption (1 d, as we checked).

1.3 Characterization

FTIR spectra were collected by a Nicolet 380 FTIR spectrometer at room temperature using the KBr method. X-ray diffraction (XRD) measurements were performed using a Phillips Xpert Pro MPD diffractometer with Cu $K\alpha$ radiation (λ=0.154 18 nm), at the room temperature, with a scanning rate of 10 °·min^{-1}, a step size of 0.0167°·s^{-1} and 2θ ranging from 4.5°~70° as well as 0.8°~6°. The generator setting is 40 kV and 40 mA. C, H and N analysis was performed in a LECO CS-444 analyzer. Zn and Al contents were analyzed using inductively coupled plasma (ICP) atomic emission spectroscopy (Jarrel-ASH, ICAP-9000). Transmission electron microscopy (TEM) images were collected using JEM-2100F (JEOL Ltd.). Scanning electron microscope (SEM) observations were carried out using a model S-4800 (Hitachi, Ltd.) operating at 5.0 kV.

2 Results and discussion

The XRD patterns (Fig.1) show that CO_3^{2-} and NO_3^- type ZnAl-LDHs crystals precursor has a hexagonal symmetry with $R\bar{3}m$ space group. The d_{003} values of CO_3^{2-} and NO_3^- type ZnAl-LDHs are 0.75 and 0.88 nm, respectively. The patterns imply that pure phase LDHs with good crystallinity have been obtained. Fig.1c shows the wet-state pattern of the NO_3^--LDHs colloidal suspension. In the pattern, only the small peak at d_{110}=0.152 nm and the amorphous halo in 2θ range of 20° ~30° are observable. This indicates that the LDHs crytals are exfoliated to 2D nanosheets, and even so, the layer is not changed remarkably.

The XRD patterns (Fig.2A and 2B) show haloes in 2θ range of 20° ~30° and 25° ~45° for the nanocomposite samples before and after water-washing, respectively. The patterns are characteristics of amorphous materials, however, for each sample a small peak at d_{110}=0.152 nm showing the existence of nanosheets is also been observed. Thus, the patterns confirm that the nanosheets exist in the samples and that CMC prevents the INS from restacking in water. The chemical formula of the INS (Table 1), $[Zn_{0.45}Al_{0.51}(OH)_2]^{0.44+}$, and the specific surface area is 1.3×10^3 $m^2\cdot g^{-1}$.

After dried, the peaks in the patterns (Fig.2C and 2D) indicate the layered structures of the nanocomposites with a large basal spacing of ~2.5 nm for the samples except for R-1/16 that contains less amounts of CMC. Taking the thickness (0.48 nm)[18] of the LDHs layer into account, the interlayer distance (Δd) of the nanocomposites is estimated to be about 2 nm. Since the size of a glucose ring in cellulose crystal is ca. 0.40 nm[19], in the large spacing, the

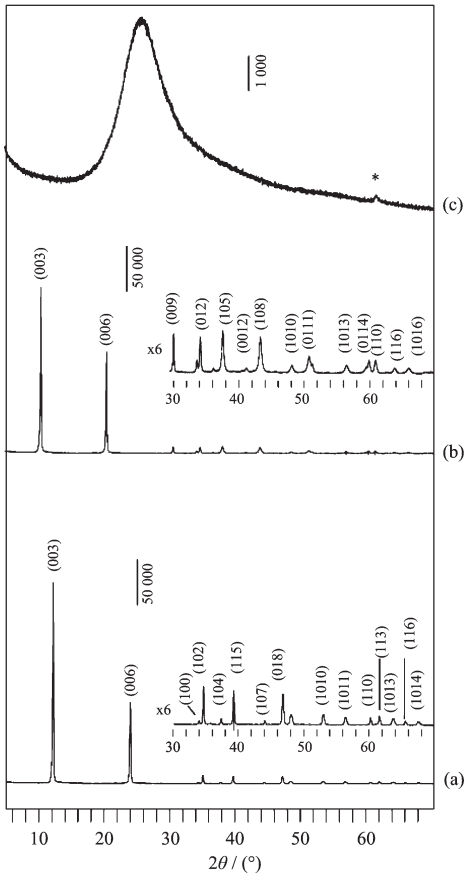

Fig.1 XRD patterns of the samples (a) CO_3^{2-}-LDHs, and (b) NO_3^--LDHs and (c) wet colloidal slurry of NO_3^- type LDHs in formamide

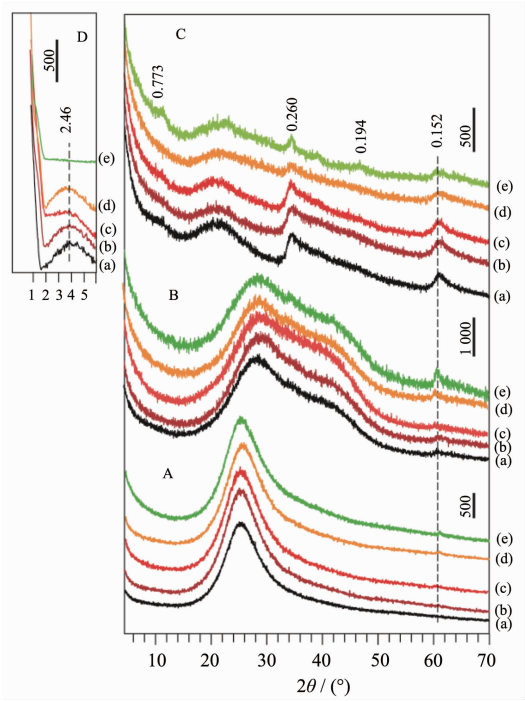

Fig.2　XRD patterns of the samples of (a) R-1, (b) R-1/2, (c) R-1/4, (d) R-1/8, and (e) R-1/16, in wet-state A: in formamide, B: in water, and C, D: dried at 40 ℃ for 12 h in vacuum; d-value in nanometers

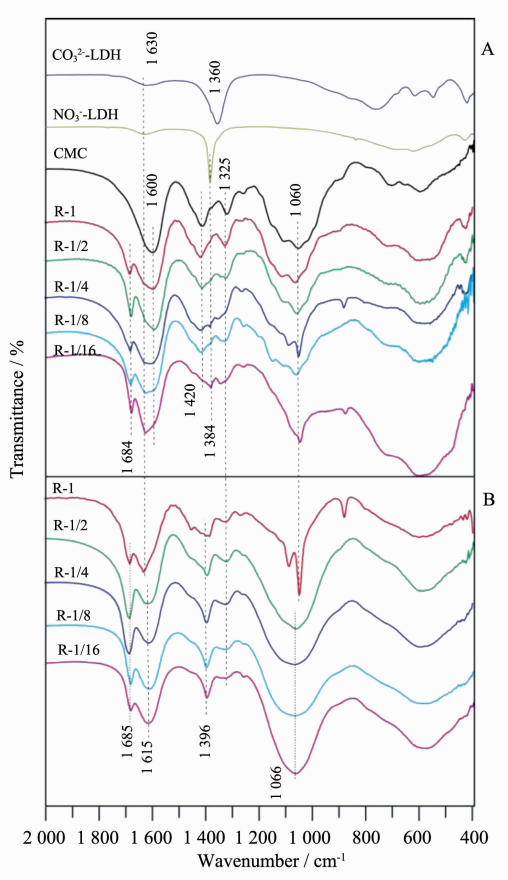

Fig.3　FTIR spectra of the samples before (A) and after (B) adsorption of phosphate

interlayer gallery could be considered as a multilayer arrangement of CMC. In the pattern of R-1/16, there is no peak in the range of high 2θ but a small peak at d =0.77 nm, which may indicate that some sheets restack to a layered structure with small spacing. In addition, a halo at 2θ 15°~30° in the patterns of the dried samples indicates the amorphous structure formed too, implying a portion of INS does not restack since they could be intertwined by CMC. This is probably the reason why almost the same basal spacing (~2.5 nm) is formed for different CMC contents. The FTIR spectra (Fig.3A) indicate the existence of CMC and LDHs. The bands at 1 420, 1 325, 1 060 cm^{-1} are characteristic of CMC [13]. The band at 1684 cm^{-1} assigned to C=O vibration for the composites appears compared with that of CMC, maybe due to the loss of sodium ion CMC. The bending vibration of O-H appears at 1 600 cm^{-1} for CMC, whereas at 1 630 cm^{-1} for LDHs. Both of the bands are observed for the composites and the latter increases in intensity, showing the relative amount decrease of CMC. Corresponding to this change, the relative intensity of 1 384 cm^{-1} band, characteristic of N=O vibration in NO_3^-, is increased for the charge compensation. No remarkable band at 1 360 cm^{-1} assigned to CO_3^{2-} is observed in the composites.

The composition of the composites (Table 1) shows that the Zn/Al molar ratio decreases markedly with the decrease of CMC. Sasaki et al.[20] considered the smaller Mg/Al ratio of MgAl-LDHs nanosheets than that of the precursor as a result of the gradual dissolution of the nanosheets in formamide. Thus the dissolution of Zn should be severer than that of Mg, and CMC exhibits an inhibitory action on the dissolution of Zn^{2+}. Compared with the designed ratio of INS/CMC, the experimental ratio is smaller for each composite. This means the loss of some nanosheets in the solid-liquid separation process, because they do not form the composite with CMC. Zn/Al ratio<1 in the LDHs implies the existence of octahedral vacancies in the layers[21], thus the Zn dissolution maybe

Table 1 Chemical composition analysis and the molar ratios of Zn/Al and INS/CMC

Sample	Composition	Zn/Al	INS/CMC	
			Des.	Expt.
LDHs*	$Zn_{0.45}Al_{0.51}(OH)_2(CO_3)_{0.07}(NO_3)_{0.30}\cdot 0.3H_2O$	0.87		
R-1	$Zn_{0.36}Al_{0.60}(OH)_2(CMC)_{0.54}(NO_3)_{0.13}\cdot 1.6H_2O$	0.60	3.1	1.9
R-1/2	$Zn_{0.28}Al_{0.60}(OH)_2(CMC)_{0.38}(NO_3)_{0.09}\cdot 1.6H_2O$	0.47	6.2	2.6
R-1/4	$Zn_{0.29}Al_{0.53}(OH)_2(CMC)_{0.18}(NO_3)_{0.05}\cdot 0.5H_2O$	0.55	12.4	5.4
R-1/8	$Zn_{0.16}Al_{0.62}(OH)_2(CMC)_{0.21}(NO_3)_{0.06}\cdot 1.4H_2O$	0.26	24.8	4.8
R-1/16	$Zn_{0.08}Al_{0.64}(OH)_2(CMC)_{0.08}(NO_3)_{0.02}\cdot 0.5H_2O$	0.12	49.6	12.8

Note: *ZnAl-LDHs INS was washed by water and then dried at 40 ℃ for 12 h in vacuum.

Des.=designed

produce more such vacancies, leading to a decrease in positive charge of the dried composites (~2.5 nm, shown in Fig.2D), which is larger than that (1.75 nm) for the composite of MgAl-LDHs and CMC[13].

The SEM images (Fig.4a) show that NO_3^--LDHs has hexagonal platelets among which the largest one is ~2 μm in size. The image for the dried composite (Fig.4b) indicates restacked LDHs plates, agreeing with the XRD diffraction peaks in Fig.2C, even though the LDHs plates become irregular on the edges and some particles become smaller after undergoing the exfoliation/restacking process. The TEM images (Fig.4c~d) of the wet sample ultrasonically dispersed in water and freeze-dried show very thin sheets of the LDHs, with wrinkles. Cellulose was not observed due to the contrast difference of the organic substance with the LDHs sheets.

Using the wet R-1 sample as adsorbent, equilibrium distribution coefficients (K_d) of different anions were determined. The K_d values of Cl^-, NO_3^-, SO_4^{2-} and $H_2PO_4^-$ are 14.8, 0.844, 29.1 and $>10^6$, respectively, showing that phosphate has much higher

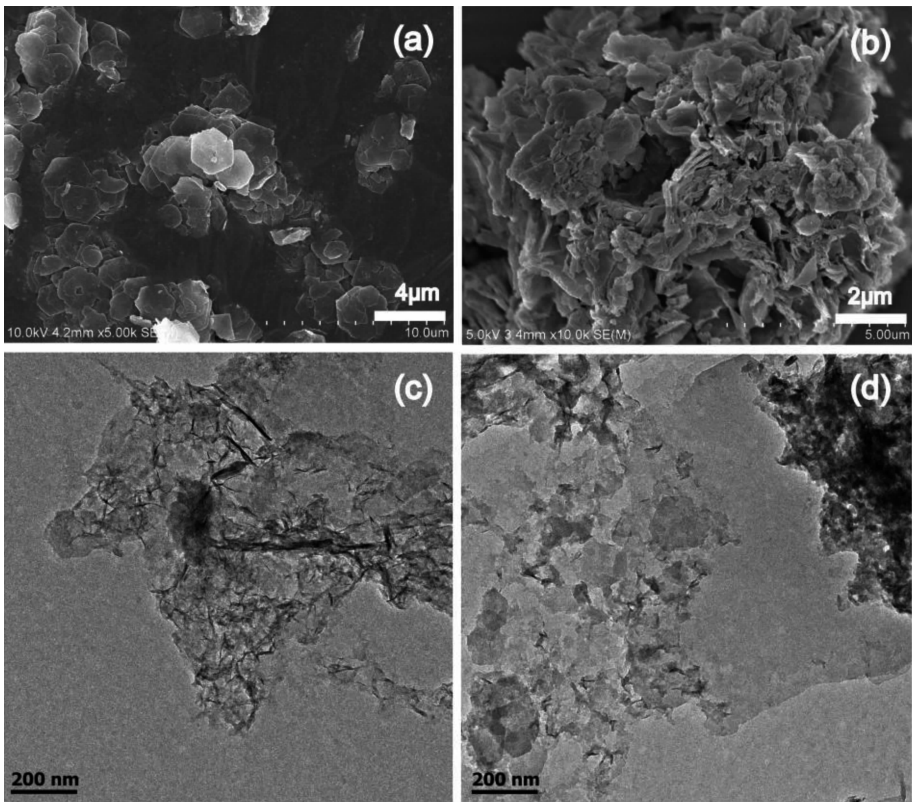

Fig.4 SEM images of (a) NO_3^--LDHs, (b) dried R-1/4, and TEM images of (c, d) wet R-1/4

K_d than other anions, and the composite has the same selectivity sequence, $H_2PO_4^- >> SO_4^{2-} > Cl^- > NO_3^-$, as the calcined LDHs products [15]. Thus, the adsorption mechanism may be also ligand complexation or electrostatic attraction between ZnO and phosphate, as we reported previously[15].

Fig.5 indicates that the adsorption capacity is larger than 26 mg (P) per gram of LDHs added, and the maximum reaches 40 mg (P) per gram of LDHs added. The value is much larger than that of the LDHs materials (16 mg (P) per gram of LDHs added) [15]. If converting the weight of LDHs to nanosheets, a maximum of 54 mg (P) per gram of LDHs added is reached by the composite. After the adsorption treatment, the pH value of the solution is changed from 5.1 to 5.9~6.1 for these samples. This pH value increase agrees with OH^- increase predicted by the adsorption mechanism mentioned above. In Fig.3B, the enveloped band at 1 066 cm^{-1} is the remarkable change after the adsorption. This change may be attributed to phosphate since the ν_3 (P-O) of phosphate would appear in the range. Another change is that 1 384 cm^{-1} (Fig.3A) becomes obscure, probably implying the ion-exchange of phosphate with NO_3^-.

As mentioned above, the INS could be intertwined by CMC via the electrostatic interaction and the hydrogen bonds between -OH groups of INS and oxygen-containing groups of CMC. This is disadvantage for INS to react with phosphate, by forming the steric hindrance, according to the mechanism of ligand complexation or electrostatic attraction ZnO and phosphate. The two inverse influences, (1) the decrease of adsorption sites due to the Zn dissolution, and (2) decrease of the steric hindrance of CMC due to the decrease of CMC content, may give rise to the maximum phosphate-adsorption in the series samples (Fig.5). Because of Zn^{2+} dissolution and the steric hindrance, the composites do not show a large adsorption amount as predicted by the high specific surface area of the INS.

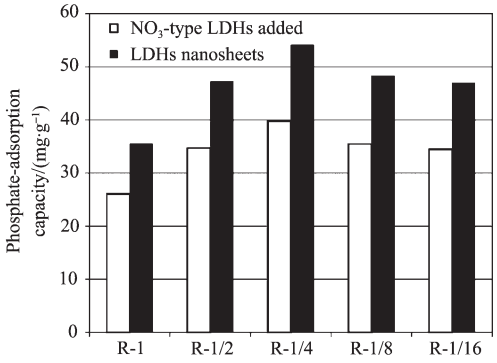

Fig.5 Phosphate-adsorption capacity based on per gram of NO_3^- type LDHs added and its equivalent LDHs nanosheets, respectively

3 Conclusions

The ZnAl-LDHs INS was stabilized in an aqueous system by forming composite with CMC, which inhibits not only restacking of INS to layered structures but also the dissolution of Zn^{2+} from INS. As an application of INS with high specific surface area, the composites obtained show high selectivity toward phosphate and highly increased phosphate-uptake amount.

Acknowledgement: This work was supported by Beijing Municipal Natural Science Foundation (No. 2112022) National Natural Science Foundation of China (NSFC No. 51172247, 5100381 and 20904064). The authors thank Drs. WU Da-Yong and CAO Jian-Hua (Technical Institute of Physics and Chemistry) and Dr. KANG Hong-Liang (Institute of Chemistry, Chinese Academy of Sciences) for their helpful discussions.

References:

[1] LEI Li-Xu(雷立旭),ZHANG Wei-Feng(张卫峰), HU Meng(胡猛), et al. *Chinese J. Inorg. Chem.* (*Wuji Huaxue Xuebao*), **2005**,**21**(4):451-463

[2] Schaak R E, Mallouk T E. *Chem. Mater.*, **2002**,**14**:1455-1471

[3] Cassagneau T, Fendler J H. *Adv. Mater.*, **1998**,**10**:877-881

[4] Hibino T, Jones W. *J. Mater. Chem.*, **2001**,**11**:1321-1323

[5] Liu Z H, Ma R Z, Sasaki T, et al. *J. Am. Chem. Soc.*, **2006**,**128**:4872-4800

[6] Osada M, Sasaki T. *J. Mater. Chem.*, **2009**,**19**:2503-2511

[7] Liu Z P, Ma R Z, Sasaki T, et al. *Langmuir*, **2007**,**23**:861-867

[8] Sakai N, Fukuda K, Omomo Y, et al. *J. Phys. Chem. C*, **2008**, **112**:5197-5202

[9] Muramatsu M, Akatsuka K, Haga M, et al. *Langmuir*, **2005**,

21:6590-6595

[10]Tanaka T, Fukuda K, Ebina Y, et al. *Adv. Mater.*, **2004**,**16**: 872-875

[11]Li L, Ma R Z, Sasaki T, et al. *J. Am. Chem. Soc.*, **2007**,**129**: 8000-8007

[12]Yan D P, Lu J, Wei M, et al. *Angew. Chem. Int. Ed.*, **2009**,**48**:3073-3076

[13]Kang H L, Ma S L, Yang X J, et al. *J. Phys. Chem. C*, **2009**, **113**:9157-9163

[14]Tezuka S, Chitrakar R, Ooi K, et al. *Bull. Chem. Soc. Jpn.*, **2004**,**77**:2101-2107

[15]He H M, Kang H L, Yang X J, et al. *J. Colloid Interface Sci.*, **2010**,**343**:225-231

[16]Goh K H, Lim T T, Dong Z. *Water Res.*, **2008**,**42**:1343-1368

[17]Tanada S, Kabayama M, Kawasaki N, et al. *J. Colloid Interface Sci.*, **2003**,**257**:135-140

[18]Newman S P, Jones W. *New J. Chem.*, **1998**,**22**:105-115

[19]Meyer K H, Mishch L. *Helv. Chim. Acta*, **1937**,**20**:232-224

[20]Ma R Z, Liu Z P, Sasaki T, et al. *J. Mater. Chem.*, **2006**,**16**: 3809-3813

[21]Ma S L, Fan C H, Yang X J, et al. *Eur. J. Inorg. Chem.*, **2010**:2079-2083